Environmental Science & Technology Letters

pubs.acs.org/journal/estlcu

Letter

Solvent-Free Nonthermal Destruction of PFAS Chemicals and PFAS in Sediment by Piezoelectric Ball Milling

Nanyang Yang,[⊥] Shasha Yang,[⊥] Qingquan Ma, Claudia Beltran, Yunqiao Guan, Madison Morsey, Elizabeth Brown, Sujan Fernando, Thomas M. Holsen, Wen Zhang, and Yang Yang*

Cite This: *Environ. Sci. Technol. Lett.* 2023, 10, 198−203

Read Online

ACCESS | Metrics & More | Article Recommendations | Supporting Information

ABSTRACT: Studies on the destruction of solid per- and polyfluoroalkyl substances (PFAS) chemicals and PFAS-laden solid wastes significantly lag behind the urgent social demand. There is a great need to develop novel treatment processes that can destroy nonaqueous PFAS at ambient temperatures and pressures. In this study, we develop a piezoelectric-material-assisted ball milling (PZM-BM) process built on the principle that ball collisions during milling can activate PZMs to generate ∼kV potentials for PFAS destruction in the absence of solvents. Using boron nitride (BN), a typical PZM, as an example, we successfully demonstrate the complete destruction and near-quantitative (∼100%) defluorination of solid PFOS and perfluorooctanoic acid (PFOA) after a 2 h treatment. This process was also used to treat PFAS-contaminated sediment. Approximately 80% of 21 targeted PFAS were destroyed after 6 h of treatment. The reaction mechanisms were determined to be a combination of piezo-electrochemical oxidation of PFAS and fluorination of BN. The PZM-BM process demonstrates many potential advantages, as the degradation of diverse PFAS is independent of functional group and chain configurations and does not require caustic chemicals, heating, or pressurization. This pioneering study lays the groundwork for optimizing PZM-BM to treat various PFAS-laden solid wastes.

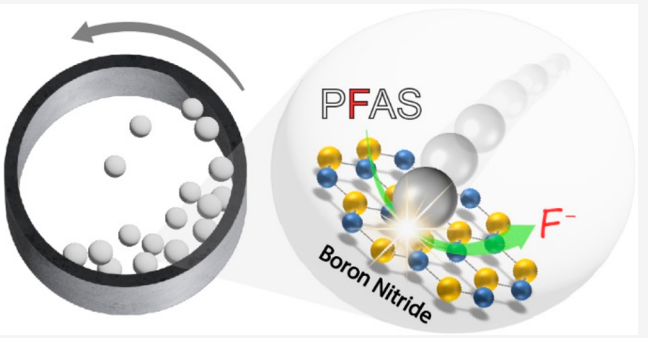

KEYWORDS: *piezoelectric material, mechanochemistry, ball milling, PFAS, sediment*

INTRODUCTION

Per- and polyfluoroalkyl substances (PFAS) are synthetic chemicals used since the 1940s.[1] Their ubiquitous presence in the environment, significant toxicity, and persistence have garnered rapidly growing public concerns.[2] Even so, the production and use of legacy PFAS, such as perfluorooctanesulfonate (PFOS) and perfluorooctanoic acid (PFOA), have not been eliminated globally.[3] Some alternative PFAS being manufactured have already shown toxicity and are facing forthcoming bans.[4,5] Therefore, the cycle of "alternative development−assessment−elimination" is a long-lasting effort that will lead to the continuous production of obsolete PFAS stockpiles. The treatment of these chemical stockpiles is extremely challenging due to the large quantity and high concentration/purity. After entering the environment, PFAS can accumulate in solid environmental matrices (i.e., sediment and soil).[6,7] Treatment of solid waste represents another challenge: the selective destruction of PFAS at lower concentrations (compared with pure chemicals) in complex solid matrices.

Landfill and incineration are two contemporary solutions for the disposal of PFAS-laden solid waste. However, landfill disposal cannot stop the re-entry of PFAS into the environment. Incineration was identified as another interim technology, as it can completely decompose PFAS.[8−10] However, the volatilization of parent PFAS and the emission of organofluorine products or perfluorinated carbons (PFCs) are still under investigation.[11,12] More importantly, the public has expressed concerns about PFAS incineration.[13] The research on the destruction of solid-state PFAS is significantly lagging behind urgent social demands and environmental needs. It is in the embryonic stage compared with the enormous efforts spent treating PFAS in water and wastewater.

Nonincineration approaches for the disposal of solid-state PFAS include ball milling (BM), hydrothermal liquefaction, and base-assisted decomposition.[14−16] Among these technologies, only BM can be operated at atmospheric temperatures and pressures to treat solids directly without solvents. To date, the destruction of selected pure PFAS compounds (PFOS,

Received: December 2, 2022
Revised: January 3, 2023
Accepted: January 4, 2023
Published: January 9, 2023

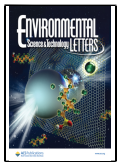

PFOA, 6:2FTS, etc.) has been demonstrated using different comilling reagents (CaO, KOH, Al_2O_3, La_2O_3, ferrate, persulfate, and SiO_2).[17−23] KOH is the only comilling reagent that achieved ∼90% conversion of fluorine on PFOS to F^-.[17,24] Although these pioneering works laid the technical groundwork, the remaining challenges must be addressed: (1) The KOH-assisted ball milling (KOH−BM) process requires excessive chemical doses.[17,22] The treated caustic solid needs to be amended before discharge/reuse. (2) Environmental humidity and moisture cause the agglomeration of KOH powders and consequently retarded reactions.[17,23] (3) Most studies have been limited to treating pure PFAS chemicals, although recently, it was implemented for treating PFAS-spiked sand and contaminated soils.[23,25]

There is a great need for alternative comilling reagents that could be as efficient as KOH in PFAS destruction and defluorination yet eliminate all the associated limitations. In this study, we report a groundbreaking piezoelectric material-assisted BM (PZM-BM) process that demonstrates effective destruction and near ∼100% defluorination of gram-level solid PFOS and PFOA. More importantly, the new process yielded a promising performance in treating PFAS-contaminated sediment.

MATERIALS AND METHODS

All chemicals were used as received and are described in Text S1. The ball milling treatment tests were performed on a planetary ball mill (PQ-N04, Across International). PFAS chemical powders or PFAS-laden sediment collected from the Schriever Air Force Base (Colorado Springs, CO) were mixed with comilling reagents (hexagonal boron nitride or KOH) in jars (100 mL) filled with balls made of stainless steel (SS) or zirconium (Zr). The jars were rotated at 580 rpm. Solid samples were taken from the jar at different intervals and subjected to solvent extraction, as detailed in Text S2, to analyze PFAS, fluoride, and other chemical components. Sample extraction, quality control, and PFAS analysis by liquid chromatography coupled to a triple quadrupole mass spectrometer (LC-MS/MS) are depicted in Text S3 and S4. Comilling reagents, alone or mixed with PFAS, were characterized by piezoelectric, infrared, and X-ray-based techniques as described in Text S5.

RESULTS AND DISCUSSION

Ball Milling Activation of Piezoelectric BN. The reported KOH−BM processes use BM to promote the nucleophilic substitution of OH^- to the carbon backbone of PFAS.[17,26] The PZM−BM process we developed operated on a different principle and was motivated by the fact that PFAS oxidation is thermodynamically feasible at high redox potential (>4 V_{RHE}) in aqueous solutions.[27,28] To realize the electrocatalytic oxidation of PFAS in solid matrices, we envision that the reaction system requires the solid−solid contact of PFAS and catalytic materials charged with high potentials.

We, therefore, theorized that piezoelectric materials (PZMs) are the ideal comilling reagent. PZMs are crystals with noncentrosymmetric structures. Upon the mechanical impact, the atomic displacement of PZMs causes a mismatch between the cation and anion centers, generating a dipole moment (Figure 1a).[29] The cumulative buildup of the dipole moments creates piezoelectric (PZ) potentials. For instance, applying stress in the normal direction (direction "3") results in polarization in the same direction (known as the 33-mode in Figure 1a). With these in mind, we hypothesize that ball collisions acting on PZMs could generate high PZ potentials to destroy PFAS.

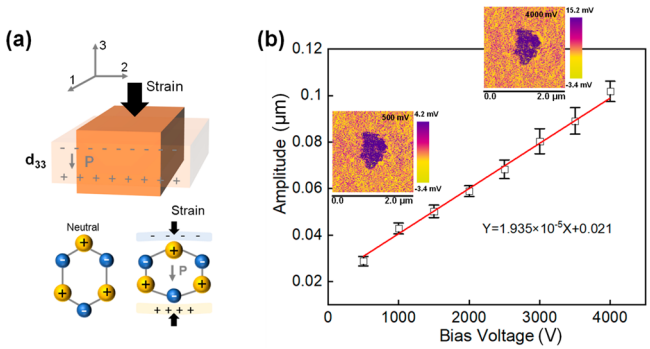

Figure 1. (a) Principle of the piezoelectric effect. A PZM crystal contains cations and anions. The overall charge of a unit cell is neutral. Upon mechanical strain-induced deformation, the cations move downward while the anions move upward. The dislocation of positive and negative charge centers results in negative and positive net charges on the top and bottom of the crystal unit cell, respectively. (b) PFM analysis of the piezoelectric response of BN under a force impact in the normal direction.

To our knowledge, the PZM−BM process has not been proposed or explored in the destruction of halogenated organic contaminants. This is the first study to validate this hypothesis using hexagonal boron nitride (BN) as a typical PZM. As revealed in Figure S1, the commercial BN sample has a particle diameter of 1−3 μm. The analysis of BN by piezoresponse force microscopy (PFM; Text S5 and Figure S2) gave the PZ coefficient under 33-mode activation, d_{33}, as 19.4 pm/V (Figure 1b), which is within the reported range (18−41 pm/V).[30,31]

Based on a general model developed for the planetary ball mill,[32,33] we also estimate the radial impact force, F_R (N), produced by the BM process under different jar rotation speeds (Figure S3). The F_R is estimated as 57 N at a jar rotation speed of 580 rpm. The PZ potential can then be estimated using the following equation:[34]

$$\mathrm{PZ} = d_{33}F_R Z/\varepsilon_0\varepsilon_r A \quad (1)$$

where $A = 1 \times 10^{-12}$ m^2 is the impact area (assuming the force acts on a 1 μm × 1 μm square BN), Z is the depth of the BN flake normal to the impact direction (30 nm, Figure S1), ε_0 is the permittivity (8.85×10^{-12} F/m), and $\varepsilon_r = 3.5$ is the relative dielectric constant of BN.[35]

Surprisingly, the theoretical calculation gives a high PZ potential of ∼3000 V. If the midpoint of the PZ potential is arbitrarily set as the Fermi level of BN (−3.6 V_{RHE}), then the 3000 V is composed of −1504 V_{RHE} cathodic potential and 1496 V_{RHE} anodic potential. The latter value readily surpasses the 4 V_{RHE} criteria for PFAS destruction. Note that the calculated value represents the ideal scenario in which a ball hits a single BN flake at the maximum impact velocity. The actual time-averaged PZ potential in a mixed powder system might vary. The real-time characterization of powders in a fast-moving jar is very challenging, so this calculated value cannot be verified in this study. However, the above calculations indicate that there may be unparalleled redox capability of BN unleashed by BM activation.

https://doi.org/10.1021/acs.estlett.2c00902
Environ. Sci. Technol. Lett. 2023, 10, 198−203

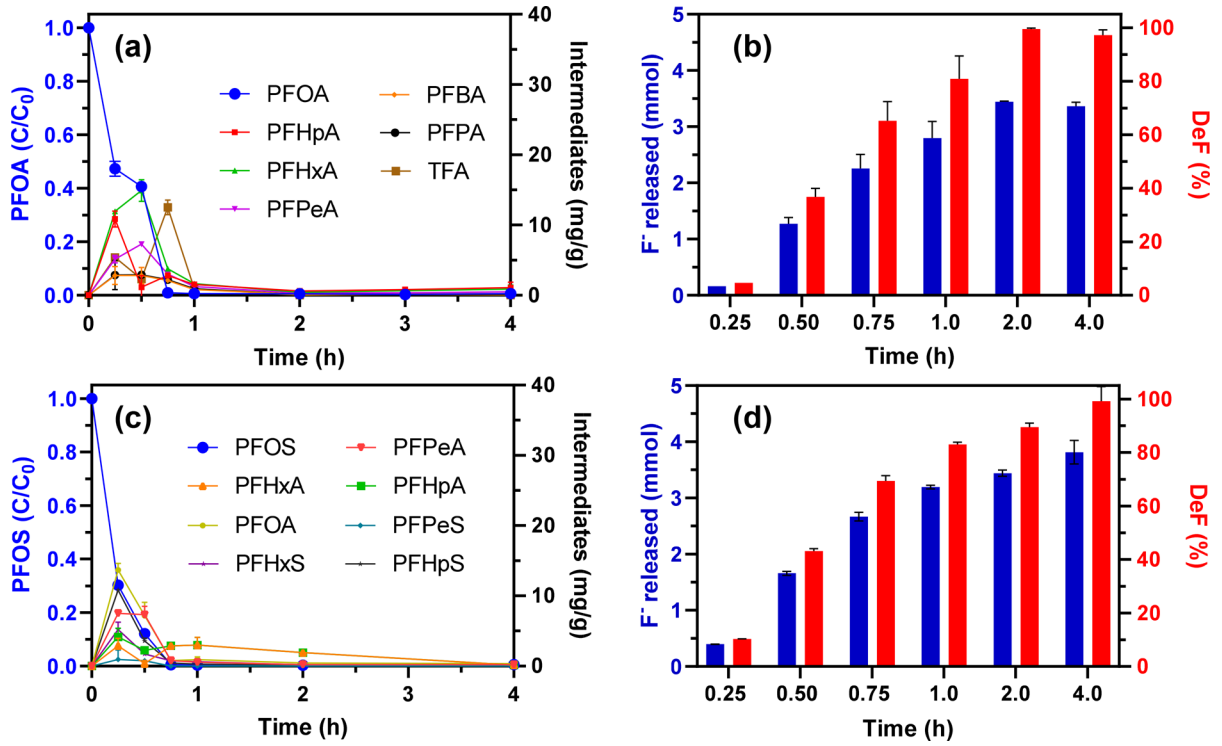

Figure 2. Destruction of (a) PFOA and (c) PFOS and formation of shorter-chain intermediates. Near-quantitative defluorination of (b) PFOA and (d) PFOS after ball milling treatment. The molar ratio of [BN] vs [F on PFAS] was set as 5:1. Specifically, 19 mmol of BN was mixed with 0.23 mmol of PFOA. For PFOS treatment, 0.23 mmol of PFOS-K was amended with 21 mmol of BN. The jar rotation speed was 580 rpm.

BN−BM Destruction and Defluorination of PFAS Chemicals. We first validated the efficacy of BN−BM in the destruction and defluorination of PFOA and PFOS solid powders. Briefly, BN powders were mixed with PFOA or PFOS and milled at 580 rpm. The [BN] vs [F on PFAS] molar ratio was optimized as 5:1 (Figures S4a and S5a). Solid samples were ultrasonically extracted by solvents to quantify PFAS and F^-. As shown in Figure 2, PFOA and PFOS were readily destroyed after 1 h. Fluoride was gradually released as one of the final products. The defluorination efficiency (DeF %) was calculated as

$$\text{DeF\%} = [F^-]/(m_0 \times n) \times 100\% \quad (2)$$

where $[F^-]$ is the fluoride molar mass detected in the extraction solution. m_0 is the molar mass of PFAS added to the jar, and n is the number of fluorine atoms on a PFAS molecule. It is critical to highlight that, for the first time, near-quantitative defluorination (i.e., DeF% = ~100%) of PFOS and PFOA was achieved after 4 h of treatment. As a comparison, the best performing KOH−BM approach could not achieve complete defluorination of PFOS, and the DeF% is between 80% and 90%.[17,24]

To unbiasedly compare the performance of two comilling reagents, we conducted parallel treatment of PFOA and PFOS using KOH−BM and BN−BM approaches. The [reagent] vs [F−PFAS] molar ratio was set as 5:1 for all reactions. The treatment was performed for 1 h. As shown in Figures S4b and S5b, the BN−BM process (100% destruction and 80% DeF%) outperformed the KOH−BM process (70% destruction; 40−50% DeF%).

Accompanied by the destruction of the parent PFAS, shorter-chain intermediates were produced and then destroyed. These results imply that the BN−BM treatment performance is independent of chain length. To exclude the contribution of metal debris (leached from SS balls) to the reaction, we used Zr balls at an equivalent total weight to substitute SS balls in the BN−BM treatment. An identical performance on PFOA and PFOS destruction and defluorination was observed (Figure S4c and S5c), suggesting that BN is the only active reagent.

Treatment of PFAS-Laden Sediments. The BN−BM process was further applied in treating PFAS in sediment. Of the 30 PFAS included in the LC−MS/MS method, 21 PFAS were detected in sediment (Table S2). The sediment was subjected to BN−BM treatment. With the increased treatment time, the gradual destruction of perfluoroalkylcarboxylic acids (PFCAs), perfluoroalkanesulfonic acids (PFSAs), and 6:2 fluorotelomer (FTS) was observed (Figure 3). The degradation kinetics are independent of chain lengths and configurations (branched vs linear). About 80% of the measured PFAS were removed after a 6 h treatment. Higher destruction efficiencies were obtained by extending the treatment to 10 h. As a comparison, the sediments were also treated by the KOH−BM process at a KOH dose equal to that of BN (20 mmol). Much slower PFAS destruction kinetics was observed compared with the BN−BM process, as the 6 h removal efficiencies for PFCA and PFSA are only 19% and 24%, respectively (Figure S6).

The ~80% destruction of PFAS after a 6 h treatment shown in Figure 3 should generate 15.1 μmol of F^-. Surprisingly, a much higher net yield of 37.2 μmol of F^- was detected in sediment after BN−BM treatment (Table S3). The sediments are impacted by aqueous film-forming foam (AFFF). Therefore, the presence of PFAS precursors beyond the 21 target PFAS detected is expected, leading to greater fluoride yield after destruction. Analyses combining combustion ion

https://doi.org/10.1021/acs.estlett.2c00902
Environ. Sci. Technol. Lett. 2023, 10, 198−203

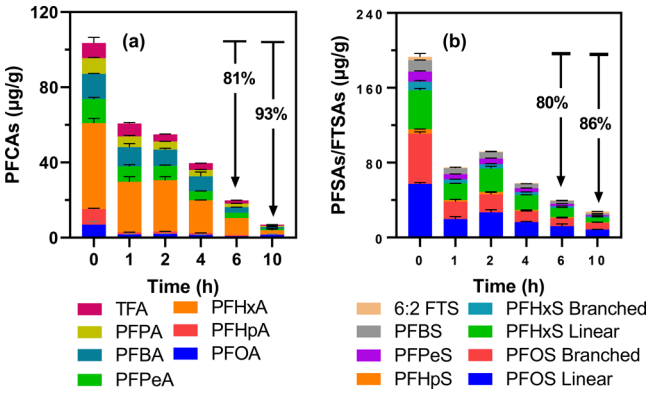

Figure 3. Destruction profiles for (a) PFCAs and (b) PFSAs/FTS in sediment with BN as the comilling reagent. Specifically, 2 g of sediment was amended with 20 mmol of BN. The jar rotation speed was 580 rpm.

chromatography (CIC) and ion chromatography (IC) show that sediment contains 70 μmol total organic fluorine (TOF)/g sediments (Table S3). A 6 h BM treatment by BN and KOH can destroy 26% and 20% of TOF, respectively. These results highlight the promise of the BN−BM process in destroying fluorocarbons that are not included in the analytical methods. They also reveal that the overall reduction of TOF is a steep challenge, which should be addressed in future studies.

Note that the moisture content of sediment is 7.8% (measured gravimetrically by oven-drying the sample at 105 °C for 24 h). Although the impact of moisture will be investigated in the forthcoming studies, the current results suggest that the BN−BM process has a higher water resistance than KOH−BM (Figure S7). Another significant advantage of BN−BM over KOH−BM is that BN−BM does not produce caustic solid waste. The extract solution (40 mL of H_2O to extract 2 g of sediment) derived from sediment treated by BN−BM has a pH of 9.9, which is significantly lower than that (pH 14.2) of sediment derived from KOH−BM (Table S3).

Mechanism Investigation. We believe the BN−BM destruction of PFAS follows the piezoelectric oxidation pathway based on the following: (1) BN can generate ∼kV PZ potentials upon the ball collision. (2) BN, as a neutral chemical, cannot induce electrophilic OH^- substitution of PFAS. (3) Radicals could be generated at high PZ potentials, but they should not be the dominant contributor to PFOA and PFOS destruction due to their high resistance to radical attack. (4) Reductive species (if any) should be readily quenched by air in the mill jar headspace. (5) The jar temperature remained <40 °C, and the BM destruction of PFAS did not occur without comilling reagents (data not shown), excluding the possibility of thermolytic destruction. (6) The formation of short-chain intermediates following the $-CF_2-$ elimination pathway was observed, identical to the patterns in electrochemical oxidation reactions.[36,37] Combining the current experimental results with the knowledge gained from electrochemical oxidation studies, we hypothesize that PFAS lose electrons to BN charged with high PZ potentials via a direct electron transfer mechanism to form fluoroalkyl radicals, which were oxidized by either oxygen or radicals (upon validation in the following studies) to form short-chain carboxylates. The steps were repeated until complete mineralization.

The BM process generated crystal defects on the BN, as evidenced by the reduced X-ray diffraction peak intensity (Figure S8). The Fourier-transform infrared spectroscopy (FTIR) characterization of the BN + PFOA mixed powder sampled during BM treatment supports the destruction of C−F and carboxylate groups (Figure S9). Further, the IR peaks associated with the bulk B−N bond remain intact, while those for the edge B−N−B structure were distorted after BM.

When 19 mmol of BN alone was milled for 2 h and then extracted by deionized (DI) water, 2.3 mmol of ammonia nitrogen (NH_3−N) was detected in the extraction solution (Table S3). Combined with the FTIR observation, these results suggest that the BM impaired edge B−N moieties, which were hydrolyzed by water. The N-sites were converted to NH_3−N. The adjacent B-sites should be concomitantly dissolved. When BN and PFOA were comilled for 2 h, XPS analysis indicated the possible formation of B−F and N−F bonds (Figure S10). Moreover, more NH_3−N (9.3 mmol) was detected in the extraction solution than when BN was milled alone.

The investigations above provided critical mechanistic insights: (1) PFAS contacts with BN were destroyed under high PZ potentials. (2) The F^- ions released from the destroyed PFAS chemically bind on the out-of-plane B- and N-sites, changing them from sp^2- to sp^3-hybridized. Such binding mechanisms have been extensively documented on fluorinated BN.[38−40] (3) After extraction by water, the fluorinated B- and N-sites, along with other edge B−N structures impaired by BM, are hydrolyzed to NH_4^+/NH_3 (pK_a = 9.26), $H_3BO/H_2BO_3^-$ (pK_{a1} = 9.15), and F^- (Figure S11). The F^- ions are readily extractable from BN, which explains the ∼100% fluoride recovery in PFOA and PFOS destruction.

It is important to highlight that BN, like many PZMs, is a semiconductor. Previously, BN was reported to be reactive for PFOA degradation in aqueous photocatalytic reactions.[41] However, there is no evidence that BN as a photocatalyst can destroy PFSAs (e.g., PFOS). We herein successfully demonstrate that the BN activated by BM could destroy PFSAs. The results imply that mechanochemical activation could bestow BN and possibly other PZMs with a stronger redox capability beyond the photocatalytic route. The broader impact of this pioneering study is validating the superior performance of the piezoelectric BM process in treating PFAS in sediments. The proof-of-concept strikes out various new paths for the following fundamental investigations on other piezoelectric materials and new applications for treating PFAS-laden solid wastes (soil, commercial products, sorbents, etc.).

■ ASSOCIATED CONTENT

Supporting Information

The Supporting Information is available free of charge at https://pubs.acs.org/doi/10.1021/acs.estlett.2c00902.

Additional experimental details, materials, and methods; images of atomic force microscopy and PFM; mathematical analysis of the BM process; data of KOH−BM treatment of PFAS chemicals and sediments; characterizations by X-ray diffraction, X-ray photoelectron spectroscopy, and FTIR; and schematic illustration of the reaction mechanisms (PDF)

■ AUTHOR INFORMATION

Corresponding Author

Yang Yang − *Department of Civil and Environmental Engineering, Clarkson University, Potsdam, New York 13699,*

https://doi.org/10.1021/acs.estlett.2c00902
Environ. Sci. Technol. Lett. 2023, 10, 198−203

United States; orcid.org/0000-0003-3767-8029; Phone: +1-315-268-3861; Email: yanyang@clarkson.edu

Authors

Nanyang Yang − *Department of Civil and Environmental Engineering, Clarkson University, Potsdam, New York 13699, United States*

Shasha Yang − *Department of Civil and Environmental Engineering and Institute for a Sustainable Environment, Clarkson University, Potsdam, New York 13699, United States*

Qingquan Ma − *John A. Reif, Jr. Department of Civil and Environmental Engineering, New Jersey Institute of Technology, Newark, New Jersey 07102, United States*

Claudia Beltran − *Department of Civil and Environmental Engineering, Clarkson University, Potsdam, New York 13699, United States*

Yunqiao Guan − *Department of Civil and Environmental Engineering, Clarkson University, Potsdam, New York 13699, United States*

Madison Morsey − *Department of Chemistry and Biomolecular Science, Clarkson University, Potsdam, New York 13699, United States*

Elizabeth Brown − *Department of Civil and Environmental Engineering, Clarkson University, Potsdam, New York 13699, United States*

Sujan Fernando − *Department of Civil and Environmental Engineering, Clarkson University, Potsdam, New York 13699, United States*

Thomas M. Holsen − *Department of Civil and Environmental Engineering, Clarkson University, Potsdam, New York 13699, United States*

Wen Zhang − *John A. Reif, Jr. Department of Civil and Environmental Engineering, New Jersey Institute of Technology, Newark, New Jersey 07102, United States;* orcid.org/0000-0001-8413-0598

Complete contact information is available at: https://pubs.acs.org/10.1021/acs.estlett.2c00902

Author Contributions

⊥N.Y. and S.Y. contributed equally.

Notes

The authors declare no competing financial interest.

■ ACKNOWLEDGMENTS

The authors are thankful for the support of the Ignite Research Fellowship of Clarkson University. The PFAS analysis is supported in part by the U.S. National Science Foundation (CBET Award 2120452).

■ REFERENCES

(1) Glüge, J.; Scheringer, M.; Cousins, I. T.; DeWitt, J. C.; Goldenman, G.; Herzke, D.; Lohmann, R.; Ng, C. A.; Trier, X.; Wang, Z. An Overview of the Uses of Per- and Polyfluoroalkyl Substances (PFAS). *Environ. Sci. Process. Impacts* **2020**, *22* (12), 2345−2373.

(2) Evich, M. G.; Davis, M. J. B.; McCord, J. P.; Acrey, B.; Awkerman, J. A.; Knappe, D. R. U.; Lindstrom, A. B.; Speth, T. F.; Tebes-Stevens, C.; Strynar, M. J.; Wang, Z.; Weber, E. J.; Henderson, W. M.; Washington, J. W. Per- and Polyfluoroalkyl Substances in the Environment. *Science* **2022**, *375* (6580), 16.

(3) Lerner, S.Teflon Toxin Goes to China. *The Intercept*, September 15, 2016. https://theintercept.com/2016/09/15/the-teflon-toxin-goes-to-china/ (accessed 2022-05-18).

(4) US EPA.*EPA Releases Updated PFBS Toxicity Assessment After Rigorous Scientific Review*. https://www.epa.gov/newsreleases/epa-releases-updated-pfbs-toxicity-assessment-after-rigorous-scientific-review-0 (accessed 2022-05-18).

(5) US EPA.*Human Health Toxicity Assessments for GenX Chemicals*. https://www.epa.gov/chemical-research/human-health-toxicity-assessments-genx-chemicals (accessed 2022-05-18).

(6) Mussabek, D.; Ahrens, L.; Persson, K. M.; Berndtsson, R. Temporal Trends and Sediment−Water Partitioning of per- and Polyfluoroalkyl Substances (PFAS) in Lake Sediment. *Chemosphere* **2019**, *227*, 624−629.

(7) Maizel, A. C.; Shea, S.; Nickerson, A.; Schaefer, C.; Higgins, C. P. Release of Per- and Polyfluoroalkyl Substances from Aqueous Film-Forming Foam Impacted Soils. *Environ. Sci. Technol.* **2021**, *55*, 14617.

(8) US EPA.*Interim Guidance on Destroying and Disposing of Certain PFAS and PFAS-Containing Materials That Are Not Consumer Products*. https://www.epa.gov/pfas/interim-guidance-destroying-and-disposing-certain-pfas-and-pfas-containing-materials-are-not (accessed 2022-02-15).

(9) Xiao, F.; Sasi, P. C.; Alinezhad, A.; Golovko, S. A.; Golovko, M. Y.; Spoto, A. Thermal Decomposition of Anionic, Zwitterionic, and Cationic Polyfluoroalkyl Substances in Aqueous Film-Forming Foams. *Environ. Sci. Technol.* **2021**, *55* (14), 9885−9894.

(10) Sasi, P. C.; Alinezhad, A.; Yao, B.; Kubátová, A.; Golovko, S. A.; Golovko, M. Y.; Xiao, F. Effect of Granular Activated Carbon and Other Porous Materials on Thermal Decomposition of Per- and Polyfluoroalkyl Substances: Mechanisms and Implications for Water Purification. *Water Res.* **2021**, *200*, 117271.

(11) Watanabe, N.; Takata, M.; Takemine, S.; Yamamoto, K. Thermal Mineralization Behavior of PFOA, PFHxA, and PFOS during Reactivation of Granular Activated Carbon (GAC) in Nitrogen Atmosphere. *Environ. Sci. Pollut. Res.* **2018**, *25* (8), 7200−7205.

(12) Wang, J.; Lin, Z.; He, X.; Song, M.; Westerhoff, P.; Doudrick, K.; Hanigan, D. Critical Review of Thermal Decomposition of Per- and Polyfluoroalkyl Substances: Mechanisms and Implications for Thermal Treatment Processes. *Environ. Sci. Technol.* **2022**, *56* (9), 5355−5370.

(13) Groups sue US military to stop PFAS incineration. *Chemical & Engineering News*, February 25, 2022. https://cen.acs.org/environment/persistent-pollutants/Groups-sue-US-military-stop/98/web/2020/02 (accessed 2022-05-18).

(14) US EPA. *Reference Guide to Non-combustion Technologies for Remediation of Persistent Organic Pollutants in Soil*, 2nd ed.; US EPA, 2010. https://www.epa.gov/remedytech/reference-guide-non-combustion-technologies-remediation-persistent-organic-pollutants (accessed 2022-05-19).

(15) Bell, L.*Non-Combustion Technology for POPs Waste Destruction: Replacing Incineration with Clean Technology*; Report for International Pollutants Elimination Network, 2021.

(16) Trang, B.; Li, Y.; Xue, X.-S.; Ateia, M.; Houk, K. N.; Dichtel, W. R. Low-Temperature Mineralization of Perfluorocarboxylic Acids. *Science* **2022**, *377* (6608), 839−845.

(17) Zhang, K.; Huang, J.; Yu, G.; Zhang, Q.; Deng, S.; Wang, B. Destruction of Perfluorooctane Sulfonate (PFOS) and Perfluorooctanoic Acid (PFOA) by Ball Milling. *Environ. Sci. Technol.* **2013**, *47* (12), 6471−6477.

(18) Yan, X.; Liu, X.; Qi, C.; Wang, D.; Lin, C. Mechanochemical Destruction of a Chlorinated Polyfluorinated Ether Sulfonate (F-53B, a PFOS Alternative) Assisted by Sodium Persulfate. *RSC Adv.* **2015**, *5* (104), 85785−85790.

(19) Lu, M.; Cagnetta, G.; Zhang, K.; Huang, J.; Yu, G. Mechanochemical Mineralization of "Very Persistent" Fluorocarbon Surfactants − 6:2 Fluorotelomer Sulfonate (6:2FTS) as an Example. *Sci. Rep.* **2017**, *7* (1), 17180.

(20) Cagnetta, G.; Huang, J.; Lu, M.; Wang, B.; Wang, Y.; Deng, S.; Yu, G. Defect Engineered Oxides for Enhanced Mechanochemical Destruction of Halogenated Organic Pollutants. *Chemosphere* **2017**, *184*, 879−883.

(21) Cagnetta, G.; Zhang, Q.; Huang, J.; Lu, M.; Wang, B.; Wang, Y.; Deng, S.; Yu, G. Mechanochemical Destruction of Perfluorinated Pollutants and Mechanosynthesis of Lanthanum Oxyfluoride: A Waste-to-Materials Process. *Chem. Eng. J.* **2017**, *316*, 1078−1090.
(22) Wang, N.; Lv, H.; Zhou, Y.; Zhu, L.; Hu, Y.; Majima, T.; Tang, H. Complete Defluorination and Mineralization of Perfluorooctanoic Acid by a Mechanochemical Method Using Alumina and Persulfate. *Environ. Sci. Technol.* **2019**, *53* (14), 8302−8313.
(23) Turner, L. P.; Kueper, B. H.; Jaansalu, K. M.; Patch, D. J.; Battye, N.; El-Sharnouby, O.; Mumford, K. G.; Weber, K. P. Mechanochemical Remediation of Perfluorooctanesulfonic Acid (PFOS) and Perfluorooctanoic Acid (PFOA) Amended Sand and Aqueous Film-Forming Foam (AFFF) Impacted Soil by Planetary Ball Milling. *Sci. Total Environ.* **2021**, *765*, 142722.
(24) Ateia, M.; Skala, L. P.; Yang, A.; Dichtel, W. R. Product Analysis and Insight into the Mechanochemical Destruction of Anionic PFAS with Potassium Hydroxide. *J. Hazard. Mater. Adv.* **2021**, *3*, 100014.
(25) Battye, N. J.; Patch, D. J.; Roberts, D. M. D.; O'Connor, N. M.; Turner, L. P.; Kueper, B. H.; Hulley, M. E.; Weber, K. P. Use of a Horizontal Ball Mill to Remediate Per- and Polyfluoroalkyl Substances in Soil. *Sci. Total Environ.* **2022**, *835*, 155506.
(26) Cagnetta, G.; Robertson, J.; Huang, J.; Zhang, K.; Yu, G. Mechanochemical Destruction of Halogenated Organic Pollutants: A Critical Review. *J. Hazard. Mater.* **2016**, *313*, 85−102.
(27) Radjenovic, J.; Sedlak, D. L. Challenges and Opportunities for Electrochemical Processes as Next-Generation Technologies for the Treatment of Contaminated Water. *Environ. Sci. Technol.* **2015**, *49* (19), 11292−11302.
(28) Yang, S.; Fernando, S.; Holsen, T. M.; Yang, Y. Inhibition of Perchlorate Formation during the Electrochemical Oxidation of Perfluoroalkyl Acid in Groundwater. *Environ. Sci. Technol. Lett.* **2019**, *6* (12), 775−780.
(29) Wang, K.; Han, C.; Li, J.; Qiu, J.; Sunarso, J.; Liu, S. The Mechanism of Piezocatalysis: Energy Band Theory or Screening Charge Effect? *Angew. Chem., Int. Ed.* **2022**, *61* (6), e202110429.
(30) Ban, C.; Jiang, X.; Li, L.; Liu, X. The Piezoelectric and Dielectric Properties of Flexible, Nanoporous, Self-Assembled Boron Nitride Nanotube Thin Films. *J. Mater. Sci.* **2019**, *54* (22), 14074−14084.
(31) Snapp, P.; Cho, C.; Lee, D.; Haque, M. F.; Nam, S.; Park, C. Tunable Piezoelectricity of Multifunctional Boron Nitride Nanotube/Poly(Dimethylsiloxane) Stretchable Composites. *Adv. Mater.* **2020**, *32* (43), 2004607.
(32) Chattopadhyay, P. P.; Manna, I.; Talapatra, S.; Pabi, S. K. A Mathematical Analysis of Milling Mechanics in a Planetary Ball Mill. *Mater. Chem. Phys.* **2001**, *68* (1), 85−94.
(33) Cagnetta, G.; Huang, J.; Wang, B.; Deng, S.; Yu, G. A Comprehensive Kinetic Model for Mechanochemical Destruction of Persistent Organic Pollutants. *Chem. Eng. J.* **2016**, *291*, 30−38.
(34) Cady, W. G.*Piezoelectricity: Vol. Two: An Introduction to the Theory and Applications of Electromechanical Phenomena in Crystals*; Courier Dover Publications, 2018.
(35) Laturia, A.; Van de Put, M. L.; Vandenberghe, W. G. Dielectric Properties of Hexagonal Boron Nitride and Transition Metal Dichalcogenides: From Monolayer to Bulk. *Npj 2D Mater. Appl.* **2018**, *2* (1), 1−7.
(36) Radjenovic, J.; Duinslaeger, N.; Avval, S. S.; Chaplin, B. P. Facing the Challenge of Poly- and Perfluoroalkyl Substances in Water: Is Electrochemical Oxidation the Answer? *Environ. Sci. Technol.* **2020**, *54* (23), 14815−14829.
(37) Niu, J.; Li, Y.; Shang, E.; Xu, Z.; Liu, J. Electrochemical Oxidation of Perfluorinated Compounds in Water. *Chemosphere* **2016**, *146*, 526−538.
(38) Radhakrishnan, S.; Das, D.; Samanta, A.; de los Reyes, C. A.; Deng, L.; Alemany, L. B.; Weldeghiorghis, T. K.; Khabashesku, V. N.; Kochat, V.; Jin, Z.; Sudeep, P. M.; Martí, A. A.; Chu, C.-W.; Roy, A.; Tiwary, C. S.; Singh, A. K.; Ajayan, P. M. Fluorinated H-BN as a Magnetic Semiconductor. *Sci. Adv.* **2017**, *3* (7), e1700842.
(39) Lai, L.; Song, W.; Lu, J.; Gao, Z.; Nagase, S.; Ni, M.; Mei, W. N.; Liu, J.; Yu, D.; Ye, H. Structural and Electronic Properties of Fluorinated Boron Nitride Nanotubes. *J. Phys. Chem. B* **2006**, *110* (29), 14092−14097.
(40) Du, M.; Li, X.; Wang, A.; Wu, Y.; Hao, X.; Zhao, M. One-Step Exfoliation and Fluorination of Boron Nitride Nanosheets and a Study of Their Magnetic Properties. *Angew. Chem., Int. Ed.* **2014**, *53* (14), 3645−3649.
(41) Duan, L.; Wang, B.; Heck, K.; Guo, S.; Clark, C. A.; Arredondo, J.; Wang, M.; Senftle, T. P.; Westerhoff, P.; Wen, X.; Song, Y.; Wong, M. S. Efficient Photocatalytic PFOA Degradation over Boron Nitride. *Environ. Sci. Technol. Lett.* **2020**, *7* (8), 613−619.

https://doi.org/10.1021/acs.estlett.2c00902
Environ. Sci. Technol. Lett. 2023, 10, 198−203